LARGE-EDDY SIMULATIONS FOR TUNDISH WITH TURBO-STOPPER FLOWS

Nouri Alkishriwi

Mechanical and Industrial Engineering Department
Faculty of Engineering, University of Tripoli, Libya
E-mail: n.alkishriwi@yahoo.com

الملخص

في هذه الورقة سيتم عرض نتائج المحاكاة للتدفق المضطرب لانسياب مصهور الحديد في الوعاء البيني الوسيط (Tundish) بأستخدام النموذج الرياضي المعروف بنمذجة الدوامات الكبيرة للأنسياب المضطرب (Large Eddy simulation of turbulent flow - LES). في هذه المحاكاة تم حل معادلات نافيير- ستوكس (Navier-Stocks equation) الخاصة بالموائع القابلة للانطغاط باستخدام التحليل العددي. تم تطوير طريقة التحليل العددي الضمني الثنائي في الزمن (Implicit Dual Time stepping scheme) اللازمة لحل المعادلات الحاكمة بحيث اشتملت على المصفوفة الشرطية (Preconditioning matrix) من جهة وطريقة التسلسل الهرمي متعدد المستويات (Multigrid Method) لتعجيل الحل من جهة أخرى. تم التحقق من صحة طريقة الحل من خلال تطبيقها على التدفق المضطرب في الأنابيب عند رقم رينولدز (محسوب عند سرعة احتكاك u_τ) يساوي 1280 ومقارنة النتائج مع البيانات التجريبية المنشورة. بعد ذلك أجريت محاكة للتدفق المضطرب لانسياب مصهور الحديد في الوعاء البيني الوسيط (Tundish) لمعرفة خصائص الانسياب ومقارنتها بالبيانات التجريبية. اظهرت نتائج المحاكة توافق جيد وإلى حد كبير مع البيانات التجريبية.

ABSTRACT

Large-eddy simulations (LES) of a continuous tundish with turbo-stoppers flows are presented. The numerical computations are performed by solving the conservation equations for compressible fluids. An implicit dual time stepping scheme combined with low Mach number preconditioning and a multigrid accelerating technique is developed for LES computations. The method is validated by comparing data of turbulent pipe flow at Re_τ=1280 at different Mach numbers with experimental findings from the literature. Finally, the characteristics of the turbulent flow in a one-strand tundish with turbo-stoppers is analyzed and discussed. The comparison of LES findings of the implicit method with experimental data from literature showed very good agreement for the mean velocity profiles and the turbulence intensity distributions in the tundish.

KEYWORDS: Turbulent Flow; Numerical Simulation; CFD; Large-Eddy Simulations

INTRODUCTION

Several approaches to study turbulent flow exist, analytical theory, experiment, and numerical simulations. Due to the nonlinearity of the governing equations, progress in analytical theory rapidly encounters limits and the analytical solutions can only be obtained for very simple cases. Experimental investigations have been conducted for many years and will remain of fundamental importance for turbulent flows. With significant progress occurring recently in computer technology growing attention is paid to the numerical simulation turbulence, which is also the approach followed in the

present work. The starting point for the numerical simulation of compressible turbulence is formed by the Navier-Stokes equations. However, turbulent flows have a wide and continuous spectrum of length and time scales to resolve, so that direct simulations of such flows are not always feasible or desirable with today's computer resources.

Large-Eddy simulation (LES) has become one of the major tools to investigate the physics of the turbulent compressible and incompressible flows. At low Mach numbers the performance of LES codes developed for the conservation equations of compressible fluids deteriorates due to the presence of two different time scales associated with acoustic and convective waves [1]. It is well known that most compressible codes do not converge to an acceptable solution when the Mach number of the flow field is smaller than $O(10^{-1})$. In many subsonic turbulent flows low Mach number regions exist, which require large integration times until a fully developed flow is established. For example low speed flows, which may be compressible due to surface heat transfer or volumetric heat addition. The numerical analysis of such flows requires solving the viscous conservation equations for compressible fluids to capture the essential effects. In such cases, the efficiency of algorithms for compressible flows can be improved considerably by low Mach number preconditioning methods. In this paper, an efficient method of solution for low subsonic flows is developed based on an implicit dual time stepping scheme combined with low Mach number preconditioning and a multigrid acceleration technique. To validate the efficiency and the accuracy of the method, large-eddy simulation of turbulent pipe flow at $Re_\tau = 1280$ is performed for several Mach numbers and the data are compared with numerical and experimental findings from the literature.

Different methods have been proposed to solve such mixed flow problems by modifying the existing compressible flow solvers. One of the most popular approaches is to use low Mach number preconditioning methods for compressible codes [1]. The basic idea of this approach is to modify the time marching behavior of the system of equations without altering the steady state solution. This is, however, only useful when the steady state solution is sought. A straightforward extension of the preconditioning approach to unsteady flow problems is achieved when it is combined with a dual time stepping technique. This idea is followed in the present paper, i.e., a highly efficient large-eddy simulation method is described based on an implicit dual time stepping scheme combined with preconditioning and multigrid. This method is validated by well known case studies [2] and finally, the preconditioned large-eddy simulation method is used to investigate the turbulent flow field in a continuous casting tundish with turbo-stopper flow problem.

The main function of a continuous casting tundish is to act as distributor of molten steel from the ladle to the moulds. The tundish plays a critical role in determining the final steel quality. In continuous casting of steel, the tundish enables to remove nonmetallic inclusions from molten steel and to regulate the flow from individual ladles to the mold Figure (1). There are two types of flow conditions in a tundish Figure (2). Steady-state casting where the mass flow rate through the shroud m_{sh} is equal to the mass flow rate through the submerged entry nozzle into the mold m_{SEN}, and transient casting in which the mass of steel in a tundish varies in time during the filling or draining stages. The motion of the liquid steel is generated by jets into the tundish and continuously casting mold. The flow regime is mostly turbulent, but some turbulence attenuation can occur far from the inlet.

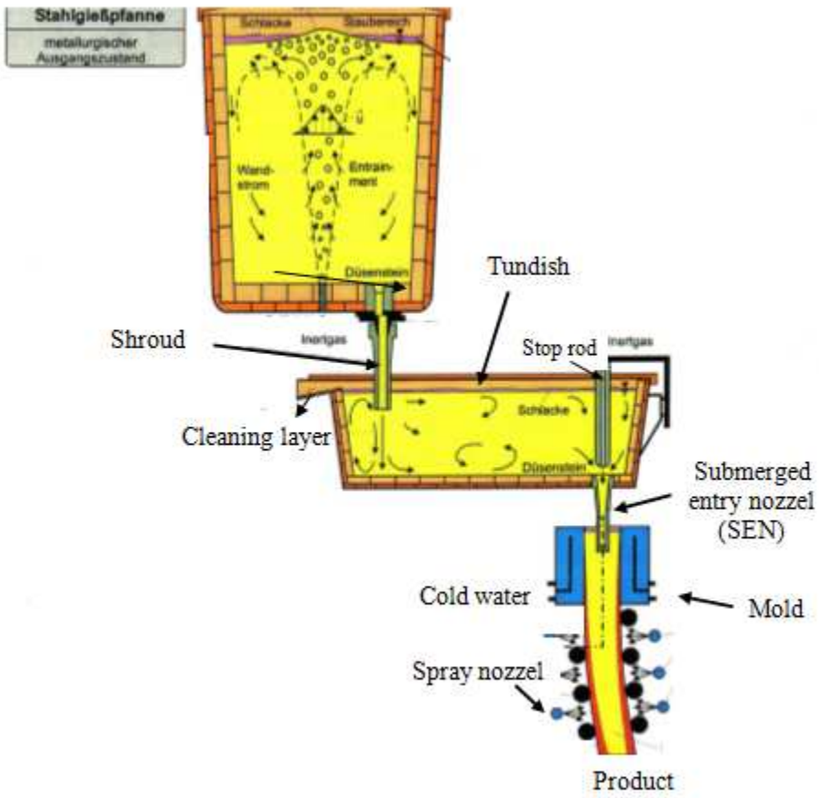

Figure 1: Principles of continuous steel casting installation. Description of tundish location in the production process

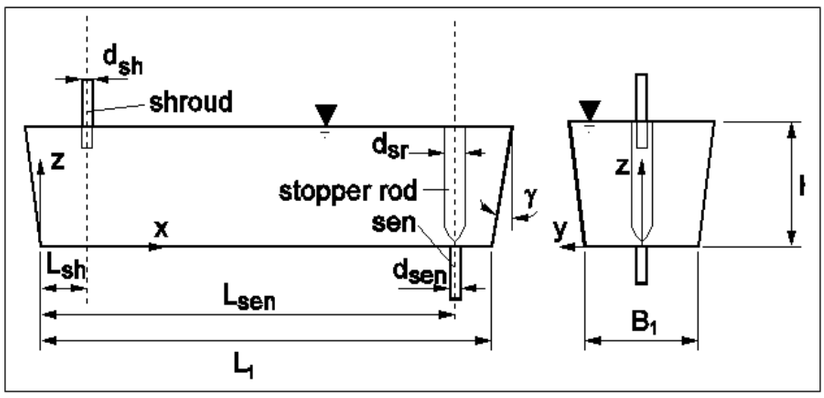

Figure 2: Presentation of the main parameters of the tundish geometry

The characteristics of the flow in a tundish include jet spreading, jet impingement on the wall, wall jets, and an important decrease of turbulence intensity in the core region of the tundish far from the jet, Gardin et al. [3]. The ladle shroud jet is rerouted at the bottom of the tundish, flows upward and generates turbulence and surface waves. The upward surge breaks up the slag cover and produces a downward surge around the

shroud. The broken flux cover allows the steel to be exposed to the atmosphere and the downward swirling shroud jet entrains particles from the slag cover within the shroud jet. The shroud jet induces a counter rotating vortex system the intensity of which decreases in the direction to the submerged entry nozzle (SEN). These vortices can draw slag into the melt and negatively affect the separation of nonmetallic particles [4]. Due to the surface waves unstable vortex structures in the mixing layer between slag and melt are induced, which suck slag into the melt.

Flow control devices for continuous casting tundish have been used for a long time to improve the cleanness of steel. Particularly turbo-stoppers (turbulence inhibitors) lead to good results because they reduce splash and surface turbulence. During steady-state casting, the turbo-stopper receives the shroud jet, redirects the stream of steel back on itself by inner lining and decelerates the upward flow resulting a reduction of surface waves. Also, the spreading conditions in the remaining tundish region are improved. In previous studies, a large amount of research has been carried out to understand the physics of the flow in a tundish mainly through numerical simulations based on the Reynolds-averaged NAVIER–STOKES (RANS) equations plus an appropriate turbulence model. To gain more knowledge about the transient turbulence process, which cannot be achieved via RANS solutions, large-eddy simulations of the tundish flow field are performed. In large-eddy simulations the large energy-containing scales of motion are simulated numerically, while the small, unresolved sub-grid scales and their interaction with the large scales are modeled. The models approximate the physics of the dynamics of the small eddies. The large scales, which usually control the behavior and statistical properties of a turbulent flow, tend to be geometry and flow dependent, whereas the small scales tend to be more universal and consequently easier to model. This fundamental advantage of LES has been used for tundish with turbo-stoppers flows.

The paper is organized as follows. After a concise presentation of the governing equations the implementation of the preconditioning in the LES context using the dual time stepping technique is described. Then, the discretization and the time marching solution technique within the dual time stepping approach are discussed. Then the numerical results of the turbulent flow in the tundish flow are presented.

GOVERNING EQUATIONS

The governing equations are the unsteady three-dimensional compressible Navier-Stokes equations written in generalized coordinates ξ_i, i=1, 2,3

$$\frac{\partial Q}{\partial t}+\frac{\partial(F_{ci}-F_{vi})}{\partial \xi_i}=0 \tag{1}$$

Where the quantity Q represents the vector of the conservative variables $(\rho,\rho u,\rho v,\rho w,\rho E)$ where ρ is the density, and u,v,w are velocity components in the three directions, and E is the total energy. The F_{ci}, F_{vi} are inviscid and viscous flux vectors, respectively. As mentioned before, preconditioning is required to provide an efficient and accurate method of solution of the steady NAVIER–STOKES equations for compressible flow at low Mach numbers. Moreover, when unsteady flows are considered, a dual-time stepping technique for time accurate solutions is used. In this approach, the solution at the next physical time step is determined as a steady-state

problem to which preconditioning, local time stepping, and multigrid are applied. Introducing of a pseudo time τ in (1), the unsteady two-dimensional governing equations with preconditioning read

$$\Gamma^{-1}\frac{\partial Q}{\partial \tau}+\frac{\partial Q}{\partial t}+R=0 \tag{2}$$

Where R represents

$$R=(\frac{\partial F_{c1}-\partial F_{v1}}{\partial \xi_1}+\frac{\partial F_{c2}-\partial F_{v2}}{\partial \xi_2}+\frac{\partial F_{c3}-\partial F_{v3}}{\partial \xi_3}) \tag{3}$$

And Γ^{-1} is the preconditioning matrix, which is to be defined such that the new eigenvalues of the preconditioned system of equations are of similar magnitude. In this study, a preconditioning technique from Turkel [1] has been implemented. It is clear that only the pseudo-time terms in (2) are altered by the preconditioning, while the physical time and space derivatives retain their original form. Convergence of the pseudo-time within each physical time step is necessary for accurate unsteady solutions. This means, the acceleration techniques such as local time stepping and multigrid can be immediately utilized to speed up the convergence within each physical time step to obtain an accurate solution for unsteady flows. The derivatives with respect to the physical time t are discretized using a three-point backward difference scheme that results in an implicit scheme, which is second-order accurate in time

$$\frac{\partial Q}{\partial \tau}=RHS \tag{4}$$

With the right-hand side

$$RHS=-\Gamma\left(\frac{3Q^{n+1}-4Q^{n}+Q^{n-1}}{2\Delta t}+R\left(Q^{n+1}\right)\right) \tag{5}$$

Note that at $\tau\rightarrow\infty$ the first term on left-hand side of (2) vanishes such that (1) is recovered. To advance the solution of the inner pseudo-time iteration, a 5-stage Runge-Kutta method in conjunction with local time stepping and multigrid is used. For stability reasons the term $3Q^{n+1}/2\Delta t$ *is* treated implicitly within the Runge-Kutta stages yielding the following formulation for the l^{th} stage

$$\begin{aligned}
&Q^{0}=Q^{n}\\
&\vdots\\
&Q^{1}=Q^{0}-\alpha_l\Delta t\left[I+\frac{3\Delta t}{2\Delta t}\alpha_l\Gamma\right]RHS \qquad (6)\\
&\vdots\\
&Q^{n+1}=Q^{5}.
\end{aligned}$$

The additional term means that in smooth flows the development in pseudo-time is proportional to the evolution in *t*.

NUMERICAL METHOD

The governing equations are the Navier-Stokes equations filtered by a low- pass filter of width Δ, which corresponds to the local average in each cell volume. Since the turbulent flow is characterized by strong interactions between various scales of motion, schemes with a large amount of artificial dissipation significantly degrade the level of energy distribution governed by the small-scale structures and therefore distort the physical representation of the dynamics of small as well as large eddies. Using a mixed central-upwind AUSM (Adjective Upstream Splitting Method) scheme with low numerical dissipation could remedy this problem. The monotone integrated large-eddy simulations (MILES) approach is used to implicitly model the small scale motions through the numerical scheme. The approximation of the convective terms of the conservation equations is based on a modified second-order accurate AUSM scheme using a centered 5-point low dissipation stencil [5] to compute the pressure derivative in the convective fluxes. The pressure term contains an additional expression, which is scaled by a weighting parameter χ that represents the rate of change of the pressure ratio with respect to the local Mach number. This parameter determines the amount of numerical dissipation to be added to avoid oscillations that could lead to unstable solutions. The parameter χ was chosen in the range $0 \leq \chi \leq 1/400$. The viscous stresses are discretized to second-order accuracy using central differences, i.e., the overall spatial approximation is second-order accurate. A dual time stepping technique is used for the temporal integration. In this approach, the solution at the next physical time step is determined as a steady state problem to which preconditioning, local time stepping and multigrid are applied. A 5-stage Runge-Kutta method is used to propagate the solution from time level n to n+1. The Runge-Kutta coeffcients are optimized for maximum stability of a centrally discretized scheme. The physical time derivative is discretized by a backward difference formula of second-order accuracy. The method is formulated for multi-block structured curvilinear grids and implemented on vector and parallel computers.

LARGE-EDDY SIMULATION OF TUNDISH FLOW

The worldwide crude steel production amounted to 1521 million tons by the end of the year 2012, 90% of which were nearly cast in continuous casting plants [6]. The continuous caster consists of ladle turret, ladle, tundish, turbo-stopper (for tundish with turbo-stopper), and oscillating mould where the liquid steel cools down and begins to solidify (see Figure 1). The steel flow, temperature distribution, and concentration of nonmetallic particles within ladle, tundish, and mould are of decisive importance for the quality of steel. The tundish regulates the flow from the ladle to the mould. It serves as a buffer and links the discontinuous process of ladle metallurgy with the continuous casting process in the mould. In addition, the tundish is designed to perform various metallurgical operations such as inclusion removal, alloy trimming of steel, calcium doped inclusion modification, superheat control, and thermal homogenization. Since the performance of tundish metallurgy operations is directly related to the nature of fluid motion, significant efforts have been made by researchers to investigate fluid flow phenomena in tundish systems. Important parameters influencing the tundish flow structure are the tundish geometry, steel level, position of the shroud, existence of turbo-stopper, and geometry of baffles, e. g., dam and weir, as well as the mass flow rates [7,8]. There are two conditions of flow in a tundish: 1) steady-state casting where the mass flow rate through the shroud is equal to the mass flow rate through the

submerged entry nozzle into the mould, and 2) transient casting conditions in which the mass of steel in a tundish varies in time during the filling or draining stages.

Experimental investigations of the melt flow in steel mills are nearly impossible due to the high temperatures and a lack of optical accessibility. Due to these difficulties physical simulations using water models are carried out. The limitations of investigations with water models concerning turbulent, non-isothermal flows, which occur in complex metallurgical processes, can be handled with computational fluid dynamics (CFD). To model the turbulence of such problems different methods are possible. These models can be classified into the approach based on the Reynolds-averaged Navier-Stokes (RANS) equations, Large-Eddy Simulation (LES) and Direct Numerical Simulation (DNS).

In large-eddy simulations the large energy-containing scales of motion are simulated numerically, while the small, unresolved subgrid scales and their interaction with the large scales are modeled. The models approximate the physics of the dynamics of the small eddies. The large scales, which usually control the behavior and statistical properties of a turbulent flow, tend to be geometry and flow dependent, whereas the small scales tend to be more universal and consequently easier to model. This fundamental advantage of LES has been used for tundish flows.

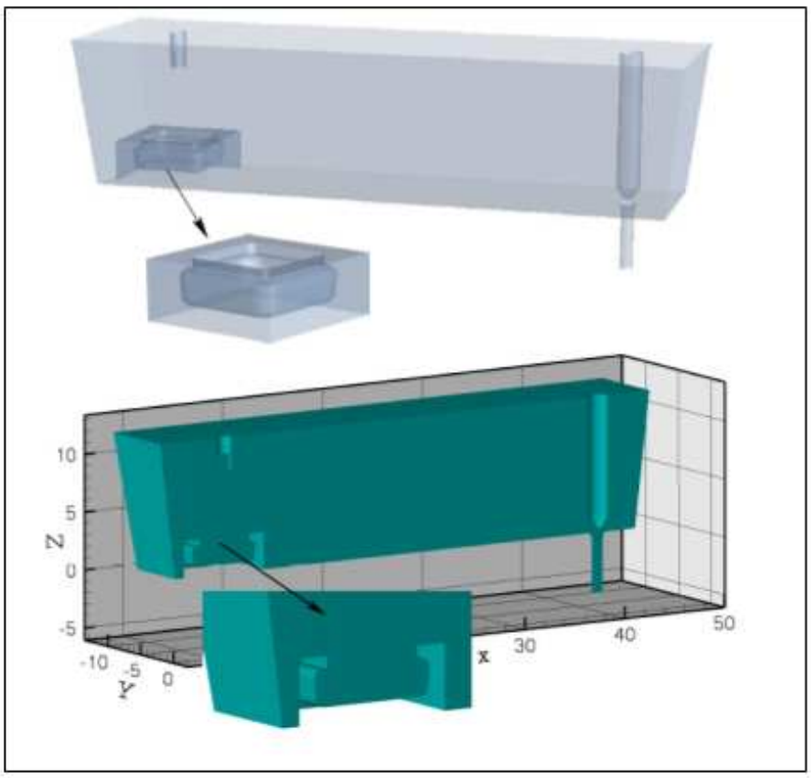

Figure 3: Description of the investigated geometry and the integration domain of the turbo-stopper of tundish.

The geometry, the flow configuration, and the main parameters for the simulation are shown in Figures (1, 2 and 3). In addition, cross-sectional pictures through the middle of the tundish with turbo-stopper describing the shape and the size of the computational domain are presented. The grid used for the simulations is shown in Figure (4). The distribution of the grid satisfies the general requirement that the grid should be smooth and refined near solid boundaries in order to obtain a higher resolution of the coherent vortices and in the jet region. The length of the computational domain of the pipe flow in the streamwise direction is 2D. The Reynolds number used in the present investigations based on the jet diameter is Re_D=25000. The minimum grid spacing used for the pipe flow and the round jet near the wall region in the radial direction is Δr^+_{min} = 1.75. In the circumferential direction, the grid spacing various linearly with r. It reaches a minimum value of $1/2(\Delta r\Delta\theta)_{min}$ = 8.1 near the centerline of the shroud of the tundish and the pipe and a maximum value $1/2(D\Delta\theta)_{max}$ =25.8 in terms of viscous wall units at the shroud wall. In the remaining part of the tundish, the maximum grid spacing in the x, y, and z-direction is Δx^+=50, Δy^+=40, and Δz^+=30 respectively. The numerical simulations consist of two simultaneously performed computations: (1) the pipe flow is calculated to provide time-dependent inflow data for the jet into the tundish (see Figure 5). (2) The flow field within the tundish is calculated. The computational domain of the flow in tundish with turbo-stopper is discretized by 14 million grid points, distributed over 40 blocks, 5 million of which are located in the jet domain to resolve the essential turbulent structures.

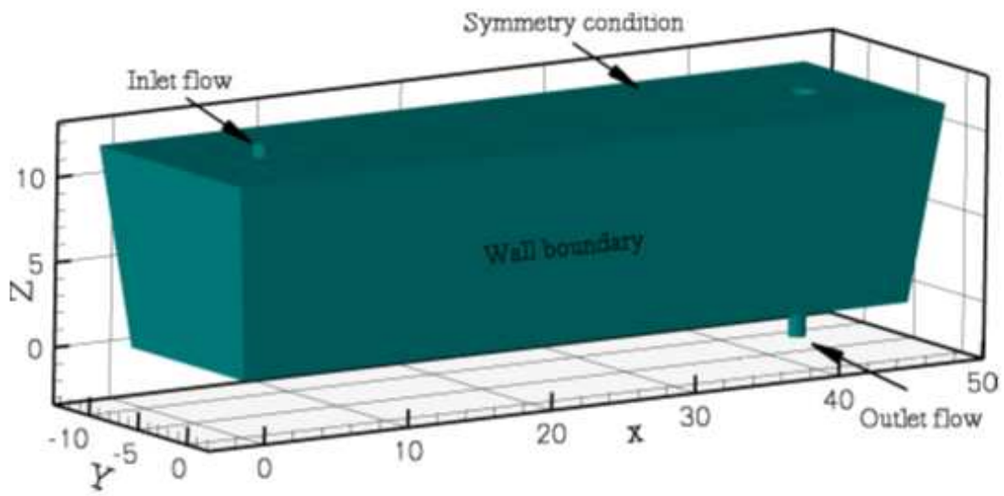

Figure 4: The types of the boundary conditions used in the tundish

Since the jet has a major impact on the flow characteristics, such as the recirculation in the center of the tundish and as such on the particle location, the interaction between the jet and the tundish flow be determined in great detail. The geometrical values and the flow parameters of the tundish are given in Table (1).

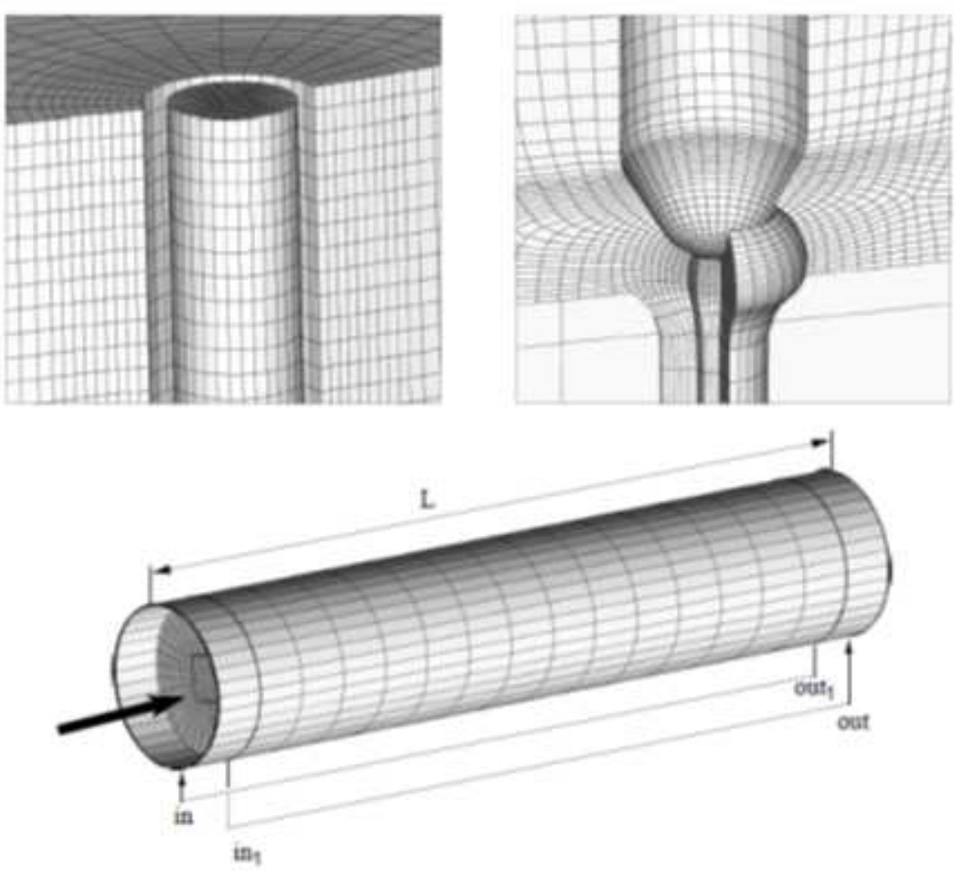

Figure 5: Computational mesh for the turbulent flow in the tundish with 14 million grid points in 40 blocks (links) and integration domain and schematic diagram of the quasiperiodic boundary conditions used for pipe flow (right)

Table 1: Physical parameters of the tundish flow

Parameter	Symbol	Value
Tundish length	L_1	1.847 m
Tundish width	B_1	0.459 m
Inclination of side walls	γ	7^o
Steel level (steady-state casting)	H	0.471 m
Position of the shroud	L_{sh}	0.197
Diameter of the shroud	d_{sh}	0.04 m
Height between bottom-shroud	Z_{sh}	0.352
Position of the SEN	L_{SEN}	1.697
Diameter of the SEN	d_{SEN}	0.041 m
Diameter of the stopper rod	d_{sr}	0.075 m
Cross section of the tundish	A	0.2431 m^2
Hydraulic diameter	d_{hyd}	0.6911 m
Volumetric flow rate		0.63 *l/s*
Quadratic turbo-stopper size	$l \times l$	0.32x0.32 m
Turbo-stopper opening size	$d \times d$	0.20x0.20 m
Re based on the jet diameter	Re_D	25000
Re based on the hydraulic diameter	Re_{dhyd}	2400

The boundary conditions of the tundish (see Figure 4) consist of no-slip conditions on solid walls. At the free surface, the normal velocity components and the normal derivatives of all remaining other variables are set zero. An LES of the impinging jet requires a prescription of the instantaneous flow variables at the inlet section of the jet.

To determine those values a slicing technique from [9] based on a simultaneously conducted LES of a fully developed turbulent pipe flow is used. The instantaneous solution in the mid-plane of the pipe flow provides the instantaneous flow variables and distributions at the inflow boundary of the jet. The boundary conditions used for pipe flow consist of no-slip and isothermal conditions on the walls. In the streamwise direction the pressure and temperature fluctuations and the mass flow are assumed to be quasi-periodic.

TUNDISH FLOW RESULTS

Large-eddy simulations of turbulent pipe flow that are simultaneously conducted to provide time dependent inflow data for the tundish problem. The Reynolds number of the simulations based on the friction velocity u_τ at $Re_\tau=u_\tau D/\nu=1280$, which corresponds to a diameter D based Reynolds number $Re_D=u_{bulk}D/\nu=25000$, where u_{bulk} is the cross-sectional average velocity. The Mach number based on the centerline velocity of the pipe is set to Ma=0.02 and the physical time step $\Delta t = 0.01$. After a fully developed turbulent pipe flow has been established the simulations are continued for another 250 dimensionless time units to compute the statistical results. Samples of the results are stored each quarter of a dimensionless time unit. Figure (6) shows the instantaneous streamwise velocity distribution with cross-flow velocity vectors. The comparison of the experimental data from [10] and pure explicit LES scheme results from [11] with the LES findings of the implicit method in Figure (7) shows very good agreement for the mean velocity profile and the turbulence intensity distributions in the pipe flow.

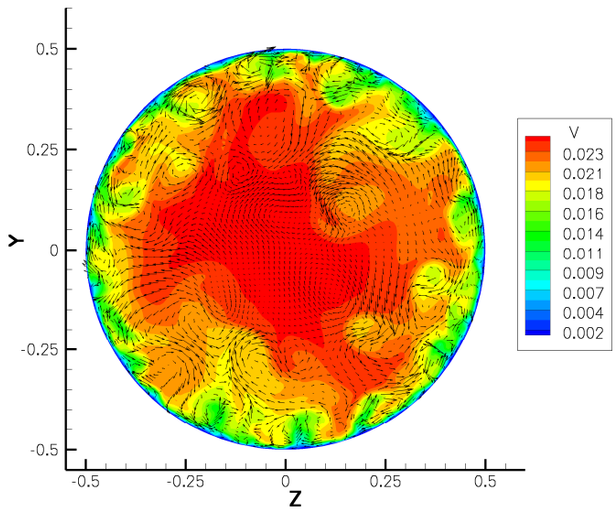

Figure :6 **LES of the fully developed turbulent pipe flow at $Re_\tau=1280$ and Ma=0.02 to provide the inflow data for the tundish simulations. Streamwise velocity distribution with cross flow velocity vectors**

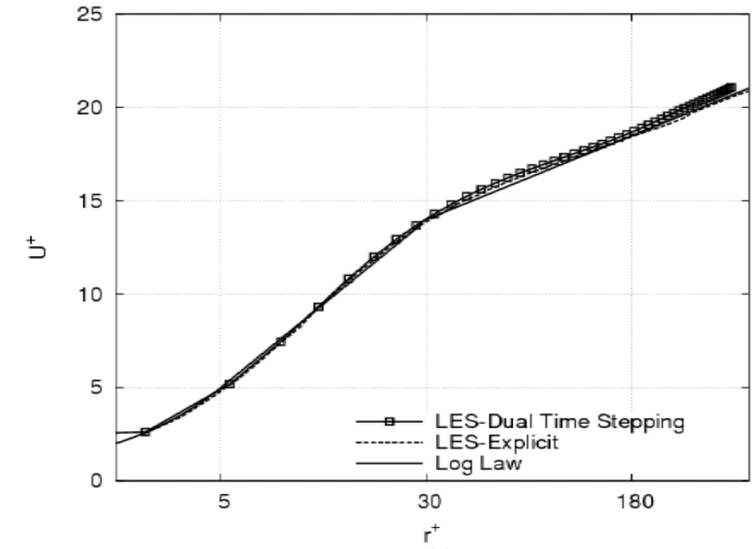

(a)

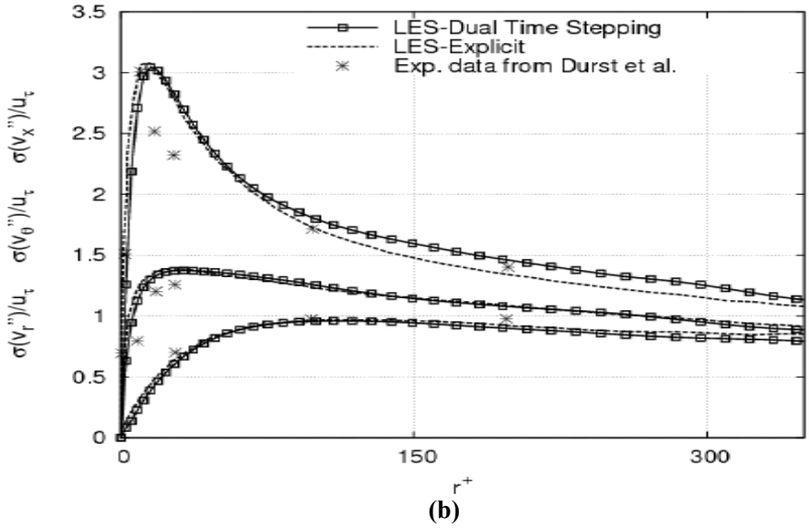

(b)

Figure 7: LES of turbulent pipe flow at Re_τ=1280 and Ma=0.02; mean velocity distributions of turbulent pipe flow U^+ vs. r^+ in inner coordinates (a); profiles of the turbulence intensities in the axial direction $\sigma(v_\infty^{"})$, the normal direction $\sigma(v_r^{"})$, and the circumferential direction $\sigma(v_\theta^{"})$, compared with experimental data from Durst et al. [10] (b). All velocities are normalized by the friction velocity u_τ

Figure (8) first, shows the jet velocity profile in the tundish close to the inlet which is 5 mm below the exit of the shroud in the tundish. Both the LES findings and the experimental data from [12] show a good agreement. Figures (9- 11) present the time-averaged velocity field and local turbulence intensity. These figures show the computed flow pattern in the longitudinal cross-sections at $y/B_1=0$ and $y/B_1=-0.5$, i.e., in the

geometrical symmetry plane, and the near side-wall plane within the tundish, respectively. They also show the flow field at x=0.1L cross-section in the x-direction.

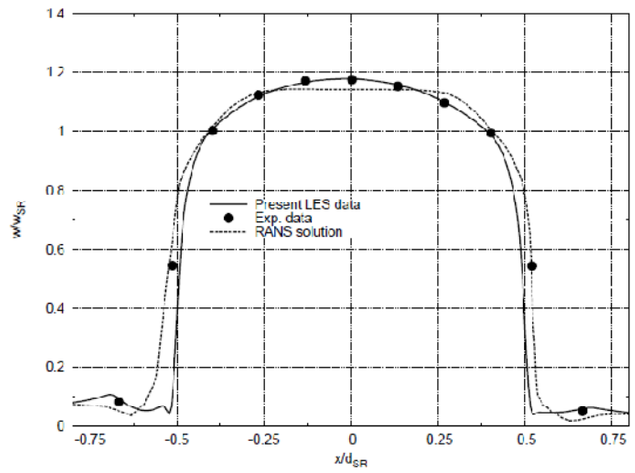

Figure 8: Large-eddy simulation of the tundish turbo-stopper. Comparison of the inlet velocity distributions at 5 mm below the shroud exit with the experimental data from [12]

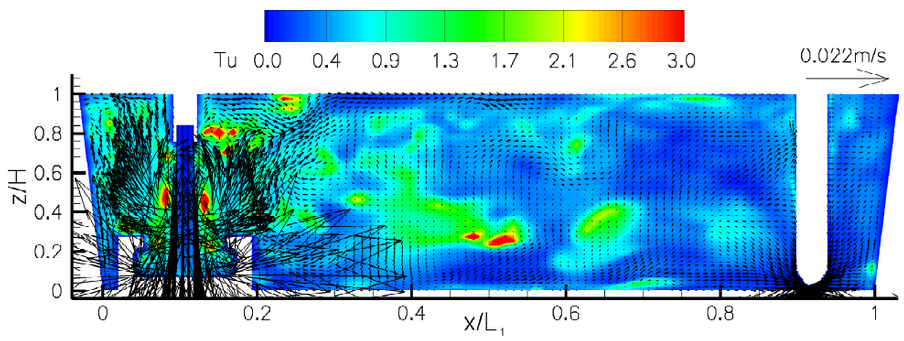

Figure 9: Large-eddy simulation of the tundish with turbo-stopper. Time averaged velocity field and local turbulence intensity at $y/B_1 = 0$, i.e., in the symmetry plane of a tundish

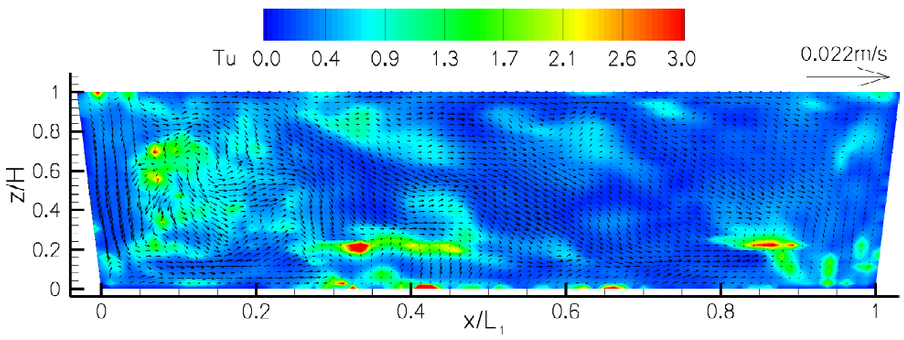

Figure 10: Large-eddy simulation of the tundish with turbo-stopper. Time averaged velocity field and local turbulence intensity at $y/B_1 = -0.5$

Unlike the tundish flow without turbo-stopper which is not presented here [13], the incoming mass flow impacts at the bottom and side walls of the turbo-stopper is redirected back on the shroud jet by the inner lining and decelerates the upward flow. Inside the turbo-stopper a quasi steady-state annular vortex develops with a size and intensity depending on the opening of the turbo-stopper. The results also show that the tundish flow can be controlled by a turbo-stopper and the flow pattern can be optimized. Because the shroud jet is redirected back on itself, turbulence is generated, and kinetic energy is dissipated within the transient shear layers and vortex system. Thereby, in the remaining tundish a more homogeneous flow is produced. Regions of high absolute turbulence are only limited to the direct inlet area of the tundish. Hence, the wave formation at the free surface is weak and the bath level is very calm compared to the tundish without turbo-stopper. Figures (11 & 12) present the vertical velocity contours and vortex structures in several horizontal planes inside and above the turbo-stopper starting from a layer near the bottom of the turbo-stopper.

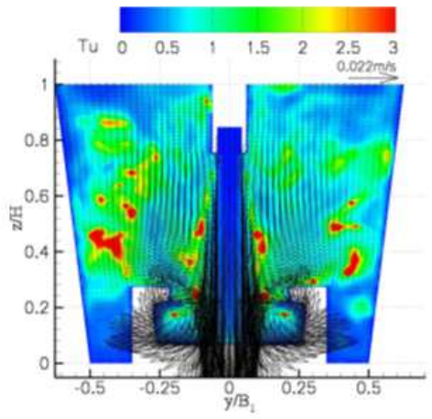

(a)

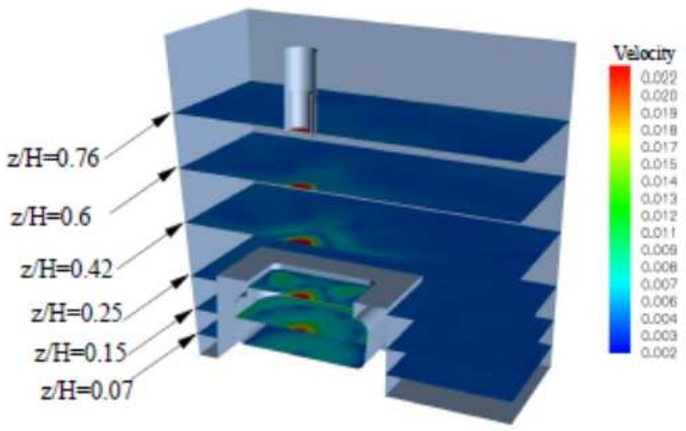

(b)

Figure 11: Large-eddy simulation of the tundish with turbo-stopper. Time averaged velocity field and local turbulence intensity at $x = 0.1L_1 = L_{sh}$ (a); time-averaged absolute velocity contours in several horizontal planes inside and above the turbo-stopper (b)

From these figures, it can be seen that the vertical speed is clearly reduced by using the turbo-stopper. This is due to the fact that the flow inside the turbo-stopper is highly three dimensional and produces an outflow above the edges of the inner lining, where the flow separates and rolls up to vortices. This type of flow field dissipates most of the kinetic energy. The vortical structures in the jet region and in the remaining part of the tundish are evidenced by the λ_2 contours in Figures (15 and 16). Again, unlike in the no-turbo-stopper case [13], the recirculation in the center of the tundish and the counter-rotating vortices are suppressed.

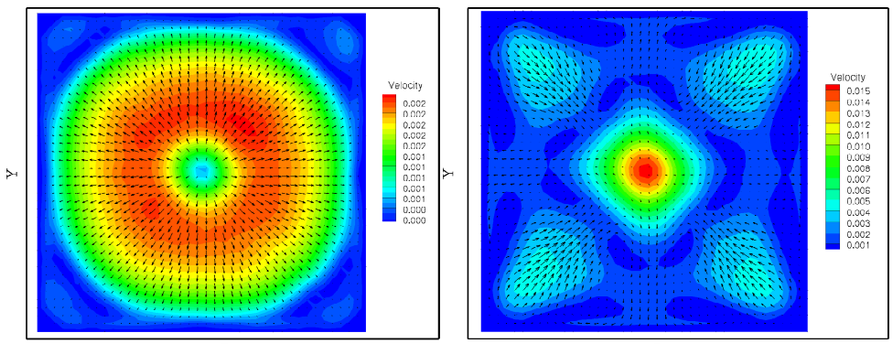

Figure 12: Large-eddy simulation of the tundish with turbo-stopper. Time-averaged velocity field at at z/H = 0.07, i.e., at the bottom of the turbo-stopper (left); z/H=0.25, i.e., inside turbo-stopper

The λ_2-criterion from Jeong and Hussain [14] is based on the decomposition of the velocity gradient tensor into a symmetric strain and an asymmetric rotation tensor.

$$\nabla \vec{u} = \begin{pmatrix} u_x & u_y & u_z \\ v_x & v_y & v_z \\ w_x & w_y & w_z \end{pmatrix} = \overline{\overline{S}} + \overline{\overline{\Omega}} \tag{7}$$

where

$$\overline{\overline{S}} = \frac{1}{2}\begin{pmatrix} 2u_x & u_y + v_x & u_z + w_x \\ v_x + u_y & 2v_y & v_z + w_y \\ w_x + u_z & w_y + v_z & 2w_z \end{pmatrix} \tag{8}$$

and

$$\overline{\overline{\Omega}} = \frac{1}{2}\begin{pmatrix} 0 & u_y + v_x & u_z - w_x \\ v_x - u_y & 0 & v_z + w_y \\ w_x - u_z & w_y - v_z & 0 \end{pmatrix} \tag{9}$$

$$\overline{\overline{M}} = \overline{\overline{S^2}} + \overline{\overline{\Omega^2}} \tag{10}$$

Jeong and Hussain found that the second negative eigenvalue λ_2 of the symmetric matrix corresponds to a local pressure minimum and closed streamline pattern. Both properties are also characteristic for a vortex pattern

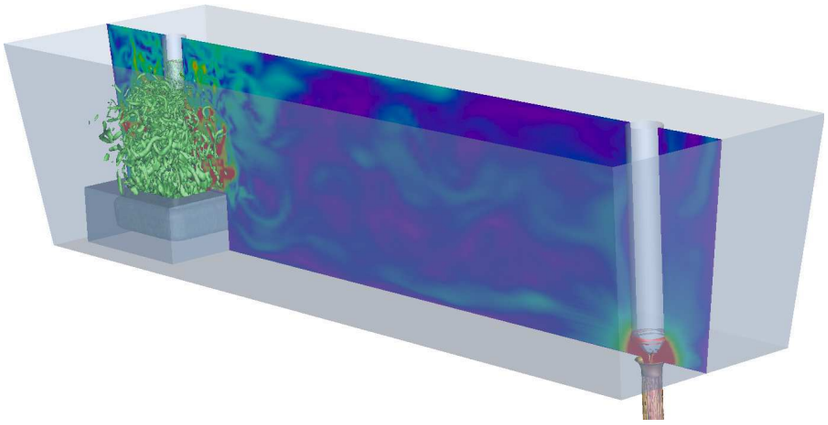

Figure 13: Large-eddy simulation of the tundish with turbo-stopper. Visualization of the vortex structure using λ_2-contours; the colors represent the velocity distribution for the instantaneous flow field in the tundish

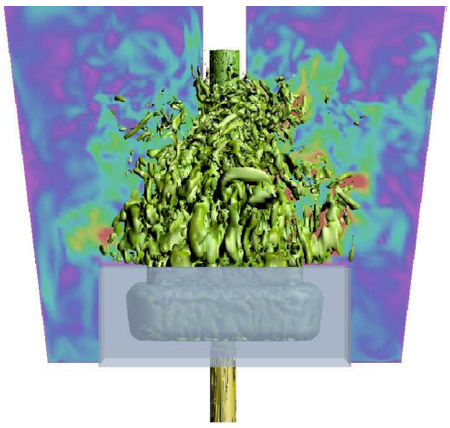

Figure 14: Visualization of the vortex structure using λ_2-contours; the colors represent the velocity distribution for the instantaneous flow field in the tundish (front view)

Conclusion

A large-eddy simulation of the flow field in a tundish with turbo-stopper is conducted to analyze the flow structure, which determines to a certain extent the steel quality. The flow pattern in a single strand tundish with and without turbo-stopper are investigated. The results showed a detailed three-dimensional turbulence structure and the comparison of the experimental data and Large-eddy simulations findings of the implicit method show very good agreement for the mean velocity profile, time averaged velocity fields, and the turbulence intensity distributions in the tundish. The results also indicated that the flow control devices, i.e., turbo-stopper device, are effective to control

the strong stirring energy within the inlet zone. Thereby, in the remaining tundish a more uniform streamlined flow is produced and such a flow pattern leads to nonmetallic removal.

REFERENCES

[1] Turkel E., Annu Rev Fluid Mech (1999) 31:385(416).

[2] Alkishriwi, N., Meinke M., and Schröder W. A large-eddy simulation method for low Mach number flows using preconditioning and multigrid. Comp. Fluids, (2006) 35/10:1126–1136.

[3] Gardin P., Brunet M., Domgin J.F., Pericleous K."An Experimental and numerical CFD study of turbulence in a tundish container". Second International Conference on CFD in the Minerals and Process Industries CSIRO, Melbourne, Australia, 6-8 December

[4] Odental H.-J., Bölling R., and Pfeifer H. Mechanism of fluid flow in a continuous casting tundish with different turbo-stoppers. J. of Steel Research (2001) 72:466–476.

[5] Meinke M., Schröder W., Krause E., Rister T. "A comparison of second- and sixth-order methods for large-eddy simulations, " Comp. & Fluids, (2002) Vol. 31, pp. 695-718

[6] World Steel Association web site.

[7] Sahai Y. and Emi T. Criteria for water modeling of melt flow and inclusion removal in continuous casting tundishes. ISIJ International, (1996) 36:1166.

[8] Sahai Y. and Emi T. Melt flow characterization in continuous casting tundishes. ISIJ International, (1996) 36:667.

[9] Breuer M. and Rodi W. Large-eddy simulation of turbulent flow through a straight square duct and an 180◦ bend. In The first ERCOFTAC Workshop on Direct and LE-Simulation. ERCOFTAC, Kluwer Academic Publishers, Mar. (1994) 36:1166.

[10] Durst F., Jovanovi´c J., and Sender J. LDA measurements in the near-wall region of a turbulent pipe flow. J. Fluid Mech. (1995) 295:305–335.

[11] Rütten F., Meinke M., and Schröder W. Large-eddy simulations of 90°-pipe bend flows. Journal of turbulence, (2001) 2:003.

[12] Bölling R. Numerische und physikalische Simulation der stationären und instationären Strömung in Stranggiessverteilern. Diss., Institut für Industrieofenbau und Wärmetechnik RWTH Aachen, Juli (2003).

[13] Alkishriwi N., Meinke M., Schröder W., Braun A., Pfeifer H. "Large-Eddy Simulations and particle-image velocimetry measurements of tundish flow". J. of Steel research, (2006) **77** No.8, pp. 565-575

[14] Jeong J. and Hussain F. On the identification of a vortex. J. Fluid Mech. (1995), 285:69–94.